Atmos. Chem. Phys. Discuss., 14, 16151–16186, 2014
www.atmos-chem-phys-discuss.net/14/16151/2014/
doi:10.5194/acpd-14-16151-2014

Atmospheric Chemistry and Physics Discussions

Fine-mode organic mass concentrations and sources in the Amazonian wet season (AMAZE-08)

Q. Chen[1,*], D. K. Farmer[2,], L. V. Rizzo[3,***], T. Pauliquevis[***], M. Kuwata[1], T. G. Karl[3,****], A. Guenther[3,*****], J. D. Allan[4], H. Coe[4], M. O. Andreae[5], U. Pöschl[5], J. L. Jimenez[2], P. Artaxo[6], and S. T. Martin[1]**

[1]School of Engineering and Applied Sciences and Department of Earth and Planetary Sciences, Harvard University, Cambridge, MA, USA
[2]Department of Chemistry and Biochemistry and Cooperative Institute for Research in Environmental Science, University of Colorado, Boulder, CO, USA
[3]National Center for Atmospheric Research, Boulder, CO, USA
[4]National Centre for Atmospheric Science and School of Earth, Atmospheric and Environmental Sciences, University of Manchester, Manchester, UK
[5]Max Planck Institute for Chemistry, Mainz, Germany
[6]Applied Physics Department and Atmospheric Science Department, University of São Paulo, São Paulo, Brazil
[*]now at: Department of Civil and Environmental Engineering, Massachusetts Institute of Technology, Cambridge, MA, USA

[**]now at: Department of Chemistry, Colorado State University, Fort Collins, CO, USA
[***]now at: Department of Exact and Earth Sciences, Federal University of São Paulo, Diadema, Brazil
[****]now at: Institute of Meteorology and Geophysics, University of Innsbruck, Austria
[*****]now at: Atmospheric Sciences and Global Change Division, Pacific Northwest National Laboratory, Richland, WA, USA

Received: 2 May 2014 – Accepted: 11 June 2014 – Published: 19 June 2014

Correspondence to: S. T. Martin (scot_martin@harvard.edu)

Published by Copernicus Publications on behalf of the European Geosciences Union.

Abstract

Real-time mass spectra of non-refractory species in submicron aerosol particles were recorded in a tropical rainforest in the central Amazon Basin during the wet season from February to March 2008, as a part of the Amazonian Aerosol Characterization Experiment (AMAZE-08). Organic material accounted on average for more than 80 % of the non-refractory submicron particle mass concentrations during the period of measurements. Ammonium was present in sufficient quantities to partially neutralize sulfate. In this acidic, isoprene-rich, HO_2-dominant environment positive-matrix factorization (PMF) of the time series of particle mass spectra identified four statistical factors to account for the 99 % variance of the signal intensities of the organic constituents: an HOA factor having a hydrocarbon-like signature and identified as regional and local pollution, an OOA-1 factor associated with long-range transport, an OOA-2 factor implicated as associated with the reactive uptake of isoprene oxidation products, especially of epoxydiols to acidic haze, fog or cloud droplets, and an OOA-3 factor consistent with the fresh production of secondary organic material (SOM) by a mechanism of gas-phase oxidation of biogenic volatile organic compounds (BVOC) followed by gas-to-particle conversion of the oxidation products. The OOA-1, -2, and -3 factors had progressively less oxidized signatures. Aqueous-phase oxidation of water-soluble products of gas-phase photochemistry might have been also involved in the formation of the OOA-2 factor. The campaign-average mass concentrations were in a ratio of 7 : 5 for the OOA-2 compared to the OOA-3 pathway, suggesting the comparable importance of particle-phase compared to gas-phase pathways for the production of SOM during the study period.

1 Introduction

Aerosol particles in the atmosphere make an important contribution to the Earth's radiation budget (IPCC, 2013). They can directly scatter and absorb shortwave and

longwave radiation, and they can indirectly affect radiative forcing and precipitation by modifying cloud properties. The assessment of the impact of human perturbations on climate requires an understanding of the natural functioning of the aerosol-cloud-climate system. During the wet season, the pristine Amazon Basin provides a unique environment for studying the sources and atmospheric evolution of natural aerosol particles and hence understanding the role of aerosol particles in biosphere-atmosphere interactions (Andreae, 2007; Martin et al., 2010a). Tropical forest emissions and long-range transport from outside of the basin are major contributors to the number and mass budgets of Amazonian aerosol particles during the wet season because regional biomass burning emission is largely suppressed by heavy rainfall (Martin et al., 2010a). The forest ecosystem emits biogenic volatile organic compounds (BVOC) that can be oxidized in the atmosphere, principally by reaction with photochemically produced hydroxyl radical and ozone molecules. Some of the oxidized products have sufficiently low vapor pressure to condense and form secondary organic material (SOM) in the particle phase. The oxidation of BVOC correlates with available sunlight, resulting in daytime increases in the particle-phase mass concentrations of typical BVOC-oxidation products, such as dicarboxylic acids (Graham et al., 2003a). In particular for Amazonia where the emission of the BVOC is dominated by isoprene, the concentrations of isoprene oxidation tracers (e.g., 2-methyltetrols and C_5-alkene triols) increase in the particle phase (Claeys et al., 2004, 2010). In addition to the biogenic SOM, the forest can also directly emit primary biological particles containing potassium, phosphorus, sugars, sugar alcohols, and fatty acids (Graham et al., 2003a; Elbert et al., 2007; Pöschl et al., 2010; Pöhlker et al., 2012). The forest also emits gases important to the particle mass concentrations of inorganic ions. Ammonia can partition from the gas phase to acidic particles (Trebs et al., 2005). Reduced sulfur gases can undergo atmospheric oxidation to produces sulfuric acid that condenses to the particle phase (Andreae et al., 1990).

The Amazonian Aerosol Characterization Experiment 2008 (AMAZE-08) investigated the sources and properties of Amazonian particles (Martin et al., 2010b). Evidence from AMAZE-08 led to the conclusion that there was a large-scale contribution

of biogenic SOM to the mass concentration of submicron aerosol particles (up to 90 %), at least during the wet season (Chen et al., 2009; Pöschl et al., 2010; Schneider et al., 2011). Primary biogenic particles enriched in potassium salts in the submicron size range were suggested as seed particles that provided surfaces for the condensation of SOM (Pöhlker et al., 2012). These bio-related particles participated in the regulation of the hydrological cycle of the forest by serving as nuclei for cloud formation and subsequent precipitation (Gunthe et al., 2009; Prenni et al., 2009). In addition to particle production tied to the forest ecosystem, lidar observations provided evidence of episodic long-range advection of African smoke and Saharan dust (Baars et al., 2011). These intrusions were temporally consistent with increases of heavily oxidized organic particles (Chen et al., 2009) indicative of long atmospheric residence times as well as increases in the concentrations of ice nuclei (Prenni et al., 2009).

Condensational growth has been reported as an important pathway of biogenic SOM production in Amazonia (Graham et al., 2003a; Chen et al., 2009). Pöhlker et al. (2012) further proposed a significant role of liquid-phase processing for Amazonian aerosol particles. Laboratory studies have demonstrated the production of organic acids and oligomers from the OH-initiated aqueous-phase oxidation of the photooxidation products of isoprene, e.g., glyoxal, methacrolein (MACR), and methylvinyl ketone (MVK) (Lim et al., 2010), as well as the acid-catalyzed reactive uptake of isoprene epoxydiol (IEPOX) isomers produced by the photooxidation of isoprene under HO_2-dominant conditions (Surratt et al., 2010; Lin et al., 2012). HO_2-dominant conditions refer to the fate of peroxy radicals with respect to reaction with HO_2 or NO. For SOM produced by these particle-phase pathways, a fraction of the mass may remain in the particle phase after dehumidification. The relative importance to SOM mass concentration of such particle-phase reaction pathways compared to gas-phase-oxidation followed by condensation is, however, still poorly understood (Martin et al., 2010a; Ervens et al., 2011). Field characterization is crucial for constraining the relative importance of different reaction pathways.

The present study analyzes multiple data sets collected during AMAZE-08 in relation to one another and in the context of the chemistry and properties of submicron particles in the Amazon Basin during the wet season. Positive-matrix factorization of the time series of particle mass spectra is used to identify statistical factors that differ in mass spectral patterns (Zhang et al., 2011). The properties of these factors, in conjunction with the auxiliary data sets, are used to investigate the relative importance of different possible sources of fine-mode organic mass concentration in Amazonia during the wet season.

2 Site and instrument description

Ground-based measurements were carried out at a rainforest site during the wet season from 7 February to 13 March 2008 (Martin et al., 2010b). The site (02°35.68′ S, 60°12.56′ W, 110 m a.s.l.) located 60 km NNW of Manaus and faced 1600 km of nearly pristine forest to the east to the Atlantic Ocean. The site was accessed by a 34 km unpaved road from Highway 174 (Supplement Fig. S1). The ten-day back trajectories indicated that during the measurement period the air masses mainly originated from the northeast over the Atlantic Ocean in the direction of Cape Verde and the Canary Islands. Air was sampled at the top of a tower ("TT34"; 38.75 m) above the forest canopy (33 m). Instrumentation deployed during AMAZE-08 is described in Martin et al. (2010b) and Sects. A and B of the Supplement.

The present study focuses mostly on statistical analysis of the data sets of an Aerodyne high-resolution Aerosol Mass Spectrometer (HR-AMS) in the context of complementary data sets of other instruments. Several non-standard aspects of the AMS analysis are summarized here in the main text. Mass concentrations were adjusted to standard temperature and pressure (noted as STP; 273.15 K and 10^5 Pa). Additional details on sampling by the AMS and data analysis are provided in Sect. A of the Supplement.

The AMS collection efficiency, corrected for undetected particle mass concentration mainly due to particle bounce on the vaporizer, was evaluated by comparison of the AMS data sets with those of other instruments. The description of other concurrent measurements and the comparisons among the measurements are provided in Sect. B of the Supplement and Supplement Fig. S2. The estimated campaign-average value of effective density (ρ_{eff}) for submicron Amazonian particles is $1390 \pm 150\,\text{kg}\,\text{m}^{-3}$ (Supplement Fig. S3), corresponding to the organic material density (ρ_{org}) of $1270 \pm 110\,\text{kg}\,\text{m}^{-3}$. Supplement Table S1 lists the regression coefficients for the multi-instrument data comparison. For a collection efficiency of unity, the AMS data agreed within measurement uncertainty with the other data sets. By comparison, the collection efficiency recommended for many other locations worldwide is 0.5 (Middlebrook et al., 2012). Images of filter samples showed that spherical organic particles, appearing as like-liquid droplets, were the main population in the submicron fraction of the ambient particle population for AMAZE-08 (Pöschl et al., 2010). This observation is consistent with the collection efficiency of unity because liquid particles do not bounce from the AMS vaporizer (Matthew et al., 2008).

Atomic ratios of oxygen-to-carbon (O : C), hydrogen-to-carbon (H : C), nitrogen-to-carbon (N : C), and sulfur-to-carbon (S : C), as well as the organic-mass-to-organic-carbon (OM : OC) ratios, were calculated from the high-resolution "W-mode" data (Aiken et al., 2008). Corrections described by Chen et al. (2011) and Canagaratna et al. (2014) were included for organic material having keto-, hydroxyl-, and acid-functionalities. These functionalities undergo thermally induced dehydration and decarboxylation on the AMS vaporizer, leading to increased values of $(CO^+)_{org} : (CO_2^+)_{org}$ and $(H_2O^+)_{org} : (CO_2^+)_{org}$ as compared to the values presented in Aiken et al. (2008).

Positive-matrix factorization (PMF; Paatero and Tapper, 1994) was conducted on the organic mass spectra of the medium-resolution "V-mode" data (m/z 12 to 220) taken to unit-mass resolution. The analysis used the PMF evaluation panel of Ulbrich et al. (2009) (version 4.2; "robust mode"). Further aspects of the analysis and output evaluation are provided in Sect. C of the Supplement. Because of the low mass

concentrations during AMAZE-08, the signal-to-noise ratios were insufficient for satisfactory PMF analysis of the high-resolution data. PMF results are reported herein for unit mass resolution.

3 Results and discussion

3.1 Mass concentrations and comparisons of data sets

Figure 1 shows time series of measurements by the AMS and other instruments during AMAZE-08. The AMS detects the non-refractory (NR) chemical components of the submicron fraction of the ambient particle population (NR-PM_1) (Fig. 1a–c). Organic material and sulfate were the two major components identified by the AMS, with correspondingly low concentrations of ammonium and negligible concentrations of nitrate and chloride. The campaign-average organic particle mass concentration was $0.76 \pm 0.23\,\mu\text{g}\,\text{m}^{-3}$, corresponding to $0.45 \pm 0.13\,\mu\text{g}\,\text{C}\,\text{m}^{-3}$ of organic carbon and an OM : OC ratio of 1.7. This concentration is lower than the range of 0.59 to $1.13\,\mu\text{g}\,\text{C}\,\text{m}^{-3}$ reported for $PM_{2.5}$ in previous wet-season campaigns (Martin et al., 2010a), explained by the differences in the sampled diameter domains. Some organic material can be present in a diameter range of 1 to 2.5 µm (Pöschl et al., 2010), which was not measured in the present study.

The campaign-average sulfate mass concentration of $0.19 \pm 0.06\,\mu\text{g}\,\text{m}^{-3}$ agreed well with the average value of $0.19 \pm 0.06\,\mu\text{g}\,\text{m}^{-3}$ measured by ion chromatography (IC) and the value of $0.21 \pm 0.04\,\mu\text{g}\,\text{m}^{-3}$ measured by particle-induced X-ray emission (PIXE) for the fine-mode (PM_2) filters. The average fine-mode sulfate mass concentrations for previous campaigns ranged from 0.17 to $0.26\,\mu\text{g}\,\text{m}^{-3}$ in the wet season, and sulfate was found predominately in the submicron range (Martin et al., 2010a). There was therefore consistency across campaigns and instruments for sulfate mass concentrations. Our data did not provide evidence for substantial contributions of organosulfate species

during AMAZE-08, at least at concentrations above uncertainty levels (see further in Sect. A of the Supplement).

Ammonium accounted for 2 % of the submicron particle mass concentration. The campaign-average mass concentration was $0.03 \pm 0.01\,\mu g\,m^{-3}$, in agreement with the average value of $0.04 \pm 0.01\,\mu g\,m^{-3}$ obtained for the fine-mode filters by the IC analysis. Chloride concentrations were transiently larger (up to $26\,ng\,m^{-3}$) during some periods, with a campaign-average concentration of $2\,ng\,m^{-3}$, which was consistent with the filter average. Nitrate had a campaign-average concentration of $7 \pm 2\,ng\,m^{-3}$. This value was greater than the average fine-mode concentration of $4 \pm 1\,ng\,m^{-3}$ measured by IC, possibly because of increased instrument uncertainties at low concentrations. Another possibility, substantial evaporative losses of nitrate during filter sampling, is not anticipated for the hygroscopic, acidic particles present during the measurement periods for the prevailing relative humidity. The AMS-measured nitrate accounted for 0.6 % of the total submicron particle mass concentration. As a test against possible significance of organonitrates (which also fragment to the NO_x^+ ions in the AMS (Farmer et al., 2010)) to results of the present study, a limiting assumption that assigns all AMS-measured nitrate to organonitrates increases the average O : C ratio by < 0.01 for the elemental analysis and corresponds to a maximum of 5 % contribution of organonitrates to the total organic particle mass concentration for an assumed molecular weight of $360\,g\,mol^{-1}$ (Chen et al., 2011). The low mass concentration of particle-phase organonitrates is expected because of the low prevailing NO_x concentrations and humid environment (Day et al., 2010; Liu et al., 2012).

Black carbon, mineral dust, and sea salt are common refractory components that are not quantified by the AMS. The multiangle absorption photometer (MAAP) instrument provides an optically based measurement of the black-carbon-equivalent (BCe) mass concentration, without size resolution (Petzold et al., 2002). The campaign-average concentration was $0.13\,\mu g\,m^{-3}$ (Fig. 1d). Under a limiting assumption that all black carbon occurred in the submicron fraction of the atmospheric particle population, this concentration corresponded to 11 % of the submicron mass concentration (inset of

Fig. 1e). The relative contribution of black carbon varied significantly during the course of AMAZE-08 (Fig. 1e), perhaps corresponding to the occasional advection of urban pollution from Manaus or biomass burning from Africa (Kuhn et al., 2010; Rizzo et al., 2013). This interpretation is supported by the covariance of BCe with sulfate.

Major fine-mode trace elements of mineral dust, including Si, Al, Fe, and Ca, had campaign-average mass concentrations of 0.12, 0.05, 0.04, and $0.01\,\mu g\,m^{-3}$, respectively, as analyzed for fine-mode filter samples by PIXE. An important source of the mineral dust was long-range transport from Africa. Previous campaigns in the Amazon found that about 20 % of the mineral dust occurred in the submicron domain (Fuzzi et al., 2007). Using this result for AMAZE-08 implies that mineral dust contributed about $0.1\,\mu g\,m^{-3}$ to the average mass concentration of the submicron particle population (Malm et al., 1994). The modified pie chart is shown in Supplement Fig. S4. The campaign-average mass concentrations of fine-mode metallic elements (V, Cr, Mn, Ni, Cu, Zn, Pb, and Mg in total of $2\,ng\,m^{-3}$) measured by PIXE were sufficiently low during AMAZE-08 to confirm the absence in the submicron particle mass concentration of significant metals from anthropogenic sources. The campaign-average mass concentration of fine-mode Na^+ measured by IC was $0.02\,\mu g\,m^{-3}$. This result suggests a minimal contribution of sea salt from Atlantic Ocean to the submicron particle mass concentration because sea salt is predominantly distributed in the supermicron domain (Fuzzi et al., 2007).

Figure 1f shows the time series of the particle light scattering coefficient measured by nephelometry at 550 nm for PM_7. The elevated scattering coefficients during 22 February to 3 March 2008 were driven by elevated mineral dust concentrations in the coarse mode, along with elevated submicron sulfate, BCe, and organic material arising from the advection of the Manaus pollution plume as well as long-range transport from Africa (Sect. B of the Supplement and Supplement Fig. S5). Other temporal maxima corresponded to increases of submicron particle mass concentration. Figure 1g shows the elemental compositions of the submicron organic material measured by the AMS. The O : C and H : C ratios, corrected as described in Canagaratna et al. (2014),

were 0.60 ± 0.16 (one standard deviation) and 1.60 ± 0.18 on average, respectively. The 10/90 quantiles were 0.42/0.75 and 1.42/1.80, respectively. The N : C ratios were 0.03 ± 0.01, similar to those observed in some urban areas (Aiken et al., 2008; Docherty et al., 2011).

Ammonium and sulfate mass concentrations had high correlation (R^2 = 0.95) during AMAZE-08 (Supplement Fig. S6). The molar ratio of $NH_4^+ : SO_4^{2-}$ was 0.80 (Fig. 2), meaning that there was insufficient ammonium to neutralize sulfate (i.e., requiring a molar ratio of 2) for the submicron particle population. Similar molar ratios have been reported in several previous studies in the central and northeast Amazon Basin (Talbot et al., 1988, 1990; Gerab et al., 1998; Graham et al., 2003b). Some of the unbalanced sulfate can be potassium sulfate (Fuzzi et al., 2007; Pöhlker et al., 2012). The fine mode mass concentration of K^+ measured by IC and PIXE was 0.03 µg m^{-3} on average. By comparison, at a deforested, pasture site in the southern parts of the Amazon Basin, the particle-phase ammonium can be enriched above sulfate concentrations and mainly balanced by organic acids (Trebs et al., 2005).

These earlier studies also examined the overall charge balance of the fine mode when including cations of Na^+, K^+, Ca^{2+}, and Mg^{2+} (Talbot et al., 1988, 1990; Gerab et al., 1998; Graham et al., 2003b). For AMAZE-08, the charge concentration of inorganic anions was nearly balanced by that of the inorganic cations for the fine mode. Specifically, the species SO_4^{2-}, NO_3^-, and Cl^- contributed 93, 5, and 2 % of the anions, respectively. The species NH_4^+, K^+, Na^+, Mg^{2+}, and Ca^{2+} contributed 40, 20, 15, 15, and 10 % of the cations, respectively.

Diel profiles of organic, sulfate, ammonium, nitrate, and chloride mass concentrations measured by the AMS are shown in Fig. 3. The temporal trends of the four species were highly correlated, with a minimum in mass concentrations near daybreak and a maximum in the afternoon. Nighttime rainfall efficiently removed particle mass concentration after local midnight, suggesting an absence of strong sources of submicron particles during the night. From the morning to the afternoon, photochemical production of SOM, convective mixing of particles from aloft, and regional advection

sustained mass concentrations, with quick recovery after daytime rainfall. Precipitation was typically local whereas advection was typically regional at a larger scale than precipitation. The decrease and the recovery as a campaign average during the afternoon resulted from frequent rain events around that time of day (e.g., Supplement Fig. S7). The organic particle mass concentration during the day increased even as temperature rose and relative humidity dropped, both of which can provide a thermodynamic driving force for the re-partitioning of semivolatile species from the particle phase to the gas phase (Pankow, 1994). Possible explanations include (1) sufficiently strong daytime production of SOM to outweigh evaporative sinks, (2) significant production of low-volatility SOM (Ervens et al., 2011; Ehn et al., 2014), or (3) slow evaporation rate of SOM (Vaden et al., 2011).

3.2 Multivariate factor analysis of the organic mass spectra

Multivariate analysis by positive-matrix factorization (PMF) of the temporal series of the organic component of the mass spectra was carried out for $12 \le m/z \le 220$ at unit-mass resolution. In overview, four statistical factors were identified and labeled as HOA, OOA-1, OOA-2, and OOA-3 (Fig. 4) (cf. Sect. C of the Supplement). The four factors HOA, OOA-1, OOA-2, and OOA-3 respectively accounted for 2, 18, 14, and 66 % of the variance in the data matrix, implying a residual variance of < 1 %. Time series of the mass concentration of each statistical factor are shown in Fig. 5. The four factors HOA, OOA-1, OOA-2, and OOA-3 represented on average 14, 14, 34, and 38 % of the organic particle mass concentration. By definition, the mass spectrum of the organic chemical component itself was at any time point a linear mix of the statistical factors, plus residual.

The HOA factor (Fig. 4a) was dominated by the ion series $C_nH_{2n+1}^+$, $C_nH_{2n-1}^+$, and $C_nH_{2n-3}^+$ (m/z 27, 29, 39, 41, 43, 55, 57, 67, 69...), similar to that reported for other locations (e.g., Zhang et al., 2005; Docherty et al., 2011; Robinson et al., 2011) and to that observed for engine exhaust (Canagaratna et al., 2004). This statistical factor is typically taken as an organic component associated with fossil fuel combustion

emissions that have not undergone substantial atmospheric oxidation. This factor was especially prevalent in the early part of the experiment. During this time period, other pollution tracers such as sulfate and NO_x were also at elevated concentrations. Regional pollution from Manaus and local emissions (e.g., nearby roads, highway, generator, and pump oil) were plausible contributors to the mass concentration of the HOA factor (Ahlm et al., 2009; Rizzo et al., 2013), which accounted for 14 % of the organic mass concentration as a campaign average. For comparison, other studies have reported that the HOA factor accounted for 0 to 21 % of the mass concentrations for remote locations and up to 53 % for urban regions (Jimenez et al., 2009).

The factors OOA-1, OOA-2, and OOA-3 were ranked by the $f_{44} : f_{43}$ ratios (high to low) and labeled based on Zhang et al. (2011), where $f_{m/z}$ represents the fractional contribution of the signal intensity at m/z to the statistical factor. The signal intensity was dominated at m/z 44 by the CO_2^+ fragment and at m/z 43 by the $C_2H_3O^+$ and $C_3H_7^+$ fragments. The $f_{44} : f_{43}$ ratio has been used in some settings as a surrogate for the extent of oxidation (i.e., "atmospheric aging") of SOM (Ng et al., 2010, 2011).

The OOA-1 factor had the feature of a singularly dominant peak at m/z 44 (Fig. 4b) and was believed to be mainly associated with long-range transport of African biomass burning. A dominant peak at m/z 44 has been linked to organic material that has undergone extensive oxidation during a prolonged atmospheric residence time (Ng et al., 2010). As described in Chen et al. (2009), organic material was delivered by long-range transport during some periods of AMAZE-08, and this material was continuously oxidized during the advection process. The source of this material was plausibly Africa biomass burning, as supported by concurrent lidar measurements (Baars et al., 2011) and satellite observations (Ben-Ami et al., 2010). South American biomass burning was much less significant during the wet season (Martin et al., 2010a). The mass concentration of the OOA-1 factor correlated with the concentrations of biomass burning tracers, such as chloride (R^2 = 0.52), potassium (R^2 = 0.35), and black carbon (R^2 = 0.43) in the submicron particle population (Fig. 5b) (Cubison et al., 2011). For comparison, the mass concentrations of the other three factors (HOA, OOA2, and

OOA-3) did not correlate with these tracers ($R^2 < 0.10$ for chloride; $R^2 < 0.02$ for potassium; and $R^2 < 0.20$ for black carbon with each of the three factors). The sulfate mass concentration was also elevated when the OOA-1 concentration was high (Fig. 1). The relative intensity of m/z 60, which is the typical marker for fresh biomass burning and attributed to the product levoglucosan, was less than the recommended threshold value of 0.35 % for background conditions (Docherty et al., 2008) (Supplement Fig. S8). As biomass burning particles become more oxidized due to ongoing atmospheric reactions downwind of African fires, the peak at m/z 60 was observed to diminish and that at m/z 44 was observed to increase (Capes et al., 2008).

Features of the OOA-2 factor included (1) a $f_{44} : f_{43}$ ratio greater than unity and (2) a prominent peak at m/z 82 distinct from adjacent ions along with elevated m/z 53 (Fig. 4c). These features were similar to those reported for the tropical rainforest of Borneo (OP3) (Robinson et al., 2011), the rural area of southwest Ontario, Canada (BAQS-Met 2007) (Slowik et al., 2011), and the downtown Atlanta (isoprene-rich), Georgia, USA (SEARCH) (Budisulistiorini et al., 2013). The OOA-2 factor of AMAZE-08 accounted for on average 34 % of the organic mass concentration, compared to 23 % for Borneo (named as the "83Fac" factor), up to 50 % for Ontario during periods of high isoprene emissions (named as the "UNKN" factor), and 33 % for Atlanta (named as the "IEPOX-OA" factor). Robinson et al. (2011) concluded that this factor derived from SOM produced by isoprene photooxidation. Lin et al. (2012) demonstrated the formation of 3-methyltetrahydrofuran-3,4-diols as a contributor to the m/z 82 signal detected by the AMS and dervied from the acid-catalyzed intramolecular rearrangement of IEPOX isomers in the particle phase. Although IEPOX was not directly measured during AMAZE-08, the time series of the OOA-2 mass concentration correlated with isoprene concentration (R^2 = 0.65) as well as with the sum concentration of first-generation isoprene oxidation products, specifically MVK + MACR (R^2 = 0.74) (Fig. 5c). Budisulistiorini et al. (2013) showed that the OOA-2 factor resembled the spectrum of the organic material produced in chamber experiments by the reactive uptake of gaseous IEPOX isomers by acidic particles, especially with respect to m/z 82.

Kuwata et al. (2014) confirmed this result in another chamber study. Uptake of isoprene IEPOX isomers depends on the liquid water content and the inorganic composition of the particles (Lin et al., 2012; Budisulistiorini et al., 2013; Nguyen et al., 2014). The atmosphere during AMAZE-08 was humid, HO_2-dominant, and isoprene-rich, with the presence of acidic submicron particles. These conditions favored the gas-phase production and the particle-phase reactive uptake of IEPOX isomers (Surratt et al., 2010), which were associated with m/z 82 by AMS characterization.

Particle-phase production pathways for secondary organic material in haze, fog, and cloud droplets can be several fold. In addition to IEPOX uptake and reaction, aqueous-phase chemistry of water-soluble products of gas-phase photochemistry can produce lower-volatility oxidized organic material, such as oxalate and dicarboxylic acids (Ervens et al., 2011). Pöhlker et al. (2012) reported an abundance of carboxylate functionalities of Amazonian particles consistent with aqueous processing. The oxidized material produced by aqueous-phase oxidation can help to explain the higher f_{44} in the OOA-2 factor compared to the mass spectra observed in laboratory experiments that studied the uptake of IEPOX isomers (Lin et al., 2012; Budisulistiorini et al., 2013; Nguyen et al., 2014). Pöhlker et al. (2012) also showed evidence of multiphase processing, i.e., a COOH-rich core and a C-OH-rich shell for single particles. The C-OH-rich shell was consistent with the production of polyols by IEPOX uptake and reaction (Lin et al., 2012). The OOA-2 factor during AMAZE-08 therefore plausibly represented the reactive uptake of IEPOX isomers and other gas-phase species by haze, fog, and cloud droplets.

The OOA-3 factor had distinct peaks at m/z 43, 55, and 91 (Fig. 4d). These features were also prominent in reference mass spectra recorded for SOM produced by oxidation of BVOCs in an environmental chamber for conditions relevant to the Amazon Basin (Fig. 6) (see further in Sect. D of the Supplement) (Shilling et al., 2009; Chen et al., 2011, 2012). In these laboratory studies, dry ammonium sulfate seed particles were used. SOM derived from isoprene (C_5) had a prominent peak at m/z 43. SOM derived from precursors of monoterpene α-pinene (C_{10}) and sesquiterpene

β-caryophyllene (C_{15}) had prominent peaks at m/z 55 and m/z 91. A linear combination of the three chamber spectra largely reproduced the OOA-3 factor (Supplement Fig. S9; 50 % isoprene SOM, 30 % α-pinene SOM, and 20 % β-caryophylene SOM). Other studies have also reported similar features for SOM derived from β-pinene and limonene as well as various tree emissions under chamber conditions (Kiendler-Scharr et al., 2009; Kostenidou et al., 2009). A plausible interpretation therefore is that the OOA-3 statistical factor was associated with freshly produced SOM similar to that produced in the chamber experiments, i.e., on a timescale of several hours by a mechanism of gas-to-particle partitioning of the BVOC oxidation products. In support of this interpretation, the temporal variation of the OOA-3 mass concentration tracked that of the BVOC concentrations (Fig. 5d). The OOA-3 factor contributed on average to about 38 % of the organic particle mass concentration.

Figure 7 shows the campaign-average diel profiles of the mass concentrations of the PMF factors. The HOA mass concentration showed a daytime minimum, suggesting the buildup of local pollution during the night and the removal by convective mixing during the day. The OOA-1 mass concentration peaked around noon without great variation throughout the day. This temporal behavior is expected for homogeneous mixing in the atmospheric column without in situ sources, i.e., as for material arriving by long-range transport. The small daytime increase was consistent with the daytime convective downward mixing of older, oxidized particles from aloft. By comparison, the OOA-2 and OOA-3 mass concentrations peaked in the early afternoon while the BVOC concentrations were high (cf. Fig. 3c of Chen et al., 2009). This temporal behavior was consistent with photochemically driven production of SOM.

Figure 8 shows the time series of fractional contribution by each of the four statistical factors identified by PMF analysis. The relative importance of processes as contributors to the organic particle mass concentration differed with time. As an example, Fig. 8 highlights two focus periods. During the first period, the average fractional contribution by the OOA-2 factor was five times greater than that of the OOA-3 factor. During the second period, by comparison, the fractional contribution by the OOA-3

factor was three times greater than that of the OOA-2 factor. The average organic mass concentrations of the two periods were 1.84 and 0.59 $\mu g\,m^{-3}$, respectively. As a campaign average, the mass fractions contributed by the OOA-2 and OOA-3 factors were approximately 1 : 1. The mass concentrations were in a ratio of 1.4 : 1.

4 Conclusions

The submicron particle mass concentration in the Amazonian rainforest during the wet season of 2008 was dominated by organic material. The environment was humid, HO_2-dominant, isoprene-rich, with the presence of acidic particles in the submicron fraction of the atmospheric aerosol. The time series of the mass spectra of the organic component of the submicron particles was analyzed by positive-matrix factorization. Four statistical factors labeled HOA, OOA-1, OOA-2, and OOA-3 were identified. The HOA factor was interpreted as representing regional and local pollution and accounted for 14 % of the organic particle mass concentration. The OOA-1 factor, accounting for another 14 % of the organic particle mass concentration, was highly oxidized and plausibly related to long-range transport of African biomass burning particles. The OOA-2 and OOA-3 factors were both interpreted as tied to the production of biogenic SOM and together accounted for > 70 % of the organic particle mass concentration (Fig. 8). The OOA-2 factor was consistent with the reactive uptake of isoprene oxidation products such as IEPOX by acidic aerosol particles, including haze, fog, and cloud droplets. The OOA-3 factor had mass spectral features of freshly formed biogenic SOM, believed to represent gas-to-particle condensation followed by oxidation of gas-phase BVOCs. According to this interpretation, the OOA-2 factor was associated with sustained particle-phase SOM production, and the OOA-3 factor was associated with sporadic, episodic SOM production by processes of gas-to-particle conversion. Processes are depicted in Fig. 9 concerning the production and further reactions of SOM.

Although multivariate statistical factors do not correspond to segregated individual chemical components (e.g., unlike molecules or families of molecules), the factors

nevertheless can be indicative of the relative importance of different atmospheric emissions and pathways. With this caveat in mind, the PMF analysis herein finds that the factor mass concentrations were, on average, in a ratio of 1.4 : 1 for the OOA-2 compared to the OOA-3 pathway and were dominated alternatively by the OOA-2 and OOA-3 components, suggesting comparable importance of gas-phase and particle-phase (including haze, fog, and cloud droplets) production of SOM during the study period.

The Supplement related to this article is available online at doi:10.5194/acpd-14-16151-2014-supplement.

Acknowledgements. Support was received from the USA National Science Foundation, the German Max Planck Society, and Brazilian CNPq and FAPESP agencies. Q. Chen acknowledges a NASA Earth and Space Science Fellowship. D. K. Farmer acknowledges a NOAA Global Change Fellowship. T. Pauliquevis acknowledges the CNPq grant 552831/2006-9. P. Artaxo acknowledges FAPESP projects 2008/58100-2, 2010/52658-1, 2011/50170-4, 2012/14437-9. We thank the INPA LBA central office in Manaus for logistical support during AMAZE. We thank J. Jayne and J. Kimmel from Aerodyne Research, Inc., J. Schneider, and S. Zorn for helping with the sampling and data quality control.

References

Ahlm, L., Nilsson, E. D., Krejci, R., Mårtensson, E. M., Vogt, M., and Artaxo, P.: Aerosol number fluxes over the Amazon rain forest during the wet season, Atmos. Chem. Phys., 9, 9381–9400, doi:10.5194/acp-9-9381-2009, 2009.

Aiken, A. C., Decarlo, P. F., Kroll, J. H., Worsnop, D. R., Huffman, J. A., Docherty, K. S., Ulbrich, I. M., Mohr, C., Kimmel, J. R., Sueper, D., Sun, Y., Zhang, Q., Trimborn, A., Northway, M., Ziemann, P. J., Canagaratna, M. R., Onasch, T. B., Alfarra, M. R., Prevot, A. S. H., Dommen, J., Duplissy, J., Metzger, A., Baltensperger, U., and Jimenez, J. L.: O/C and OM/OC ratios of primary, secondary, and ambient organic aerosols with high-resolution time-of-flight aerosol mass spectrometry, Environ. Sci. Technol., 42, 4478–4485, doi:10.1021/es703009q, 2008.

Andreae, M. O.: Aerosols before pollution, Science, 315, 50–51, doi:10.1126/science.1136529, 2007.

Andreae, M. O., Berresheim, H., Bingemer, H., Jacob, D. J., Lewis, B. L., Li, S. M., and Talbot, R. W.: The atmospheric sulfur cycle over the Amazon Basin. 2. Wet season, J. Geophys. Res., 95, 16813–16824, 1990.

Baars, H., Ansmann, A., Althausen, D., Engelmann, R., Artaxo, P., Pauliquevis, T., and Souza, R.: Further evidence for significant smoke transport from Africa to Amazonia, Geophys. Res. Lett., 38, L20802, doi:10.1029/2011GL049200, 2011.

Ben-Ami, Y., Koren, I., Rudich, Y., Artaxo, P., Martin, S. T., and Andreae, M. O.: Transport of North African dust from the Bodélé depression to the Amazon Basin: a case study, Atmos. Chem. Phys., 10, 7533–7544, doi:10.5194/acp-10-7533-2010, 2010.

Budisulistiorini, S. H., Canagaratna, M. R., Croteau, P. L., Marth, W. J., Baumann, K., Edgerton, E. S., Shaw, S. L., Knipping, E. M., Worsnop, D. R., Jayne, J. T., Gold, A., and Surratt, J. D.: Real-time continuous characterization of secondary organic aerosol derived from isoprene epoxydiols in downtown Atlanta, Georgia, using the Aerodyne Aerosol Chemical Speciation Monitor, Environ. Sci. Technol., 47, 5686–5694, doi:10.1021/es400023n, 2013.

Canagaratna, M. R., Jayne, J. T., Ghertner, D. A., Herndon, S., Shi, Q., Jimenez, J. L., Silva, P. J., Williams, P., Lanni, T., Drewnick, F., Demerjian, K. L., Kolb, C. E., and Worsnop, D. R.: Chase studies of particulate emissions from in-use New York City vehicles, Aerosol Sci. Technol., 38, 555–573, doi:10.1080/02786820490465504, 2004.

Canagaratna, M. R., Jimenez, J. L., Chen, Q., Massoli, P., Kessler, S., Hildebrandt, L., Fortner, E., Williams, L., Wilson, K., Surratt, J., Donahue, N. M., Kroll, J. H., Jayne, J., and Worsnop, D. R.: Improved calibration of O/C and H/C ratios obtained by Aerosol Mass Spectrometry of organic species, in preparation, 2014.

Capes, G., Johnson, B., McFiggans, G., Williams, P. I., Haywood, J., and Coe, H.: Aging of biomass burning aerosols over West Africa: aircraft measurements of chemical composition, microphysical properties, and emission ratios, J. Geophys. Res., 113, D00C15, doi:10.1029/2008jd009845, 2008.

Chen, Q., Farmer, D. K., Schneider, J., Zorn, S. R., Heald, C. L., Karl, T. G., Guenther, A., Allan, J. D., Robinson, N., Coe, H., Kimmel, J. R., Pauliquevis, T., Borrmann, S., Poschl, U., Andreae, M. O., Artaxo, P., Jimenez, J. L., and Martin, S. T.: Mass spectral characterization of submicron biogenic organic particles in the Amazon Basin, Geophys. Res. Lett., 36, L20806, doi:10.1029/2009gl039880, 2009.

Chen, Q., Liu, Y., Donahue, N. M., Shilling, J. E., and Martin, S. T.: Particle-phase chemistry of secondary organic material: modeled compared to measured O : C and H : C elemental ratios provide constraints, Environ. Sci. Technol., 45, 4763–4770, doi:10.1021/es104398s, 2011.

Chen, Q., Li, Y. L., McKinney, K. A., Kuwata, M., and Martin, S. T.: Particle mass yield from β-caryophyllene ozonolysis, Atmos. Chem. Phys., 12, 3165–3179, doi:10.5194/acp-12-3165-2012, 2012.

Claeys, M., Graham, B., Vas, G., Wang, W., Vermeylen, R., Pashynska, V., Cafmeyer, J., Guyon, P., Andreae, M. O., Artaxo, P., and Maenhaut, W.: Formation of secondary organic aerosols through photooxidation of isoprene, Science, 303, 1173–1176, doi:10.1126/science.1092805, 2004.

Claeys, M., Kourtchev, I., Pashynska, V., Vas, G., Vermeylen, R., Wang, W., Cafmeyer, J., Chi, X., Artaxo, P., Andreae, M. O., and Maenhaut, W.: Polar organic marker compounds in atmospheric aerosols during the LBA-SMOCC 2002 biomass burning experiment in Rondônia, Brazil: sources and source processes, time series, diel variations and size distributions, Atmos. Chem. Phys., 10, 9319–9331, doi:10.5194/acp-10-9319-2010, 2010.

Cubison, M. J., Ortega, A. M., Hayes, P. L., Farmer, D. K., Day, D., Lechner, M. J., Brune, W. H., Apel, E., Diskin, G. S., Fisher, J. A., Fuelberg, H. E., Hecobian, A., Knapp, D. J., Mikoviny, T., Riemer, D., Sachse, G. W., Sessions, W., Weber, R. J., Weinheimer, A. J., Wisthaler, A., and Jimenez, J. L.: Effects of aging on organic aerosol from open biomass burning smoke in aircraft and laboratory studies, Atmos. Chem. Phys., 11, 12049–12064, doi:10.5194/acp-11-12049-2011, 2011.

Day, D. A., Liu, S., Russell, L. M., and Ziemann, P. J.: Organonitrate group concentrations in submicron particles with high nitrate and organic fractions in coastal southern California, Atmos. Environ., 44, 1970–1979, doi:10.1016/j.atmosenv.2010.02.045, 2010.

Docherty, K. S., Stone, E. A., Ulbrich, I. M., DeCarlo, P. F., Snyder, D. C., Schauer, J. J., Peltier, R. E., Weber, R. J., Murphy, S. M., Seinfeld, J. H., Grover, B. D., Eatough, D. J., and Jimenez, J. L.: Apportionment of primary and secondary organic aerosols in southern California during the 2005 Study of Organic Aerosols in Riverside (SOAR-1), Environ. Sci. Technol., 42, 7655–7662, doi:10.1021/es8008166, 2008.

Docherty, K. S., Aiken, A. C., Huffman, J. A., Ulbrich, I. M., DeCarlo, P. F., Sueper, D., Worsnop, D. R., Snyder, D. C., Peltier, R. E., Weber, R. J., Grover, B. D., Eatough, D. J., Williams, B. J., Goldstein, A. H., Ziemann, P. J., and Jimenez, J. L.: The 2005 Study

of Organic Aerosols at Riverside (SOAR-1): instrumental intercomparisons and fine particle composition, Atmos. Chem. Phys., 11, 12387–12420, doi:10.5194/acp-11-12387-2011, 2011.

Ehn, M., Thornton, J. A., Kleist, E., Sipila, M., Junninen, H., Pullinen, I., Springer, M., Rubach, F., Tillmann, R., Lee, B., Lopez-Hilfiker, F., Andres, S., Acir, I. H., Rissanen, M., Jokinen, T., Schobesberger, S., Kangasluoma, J., Kontkanen, J., Nieminen, T., Kurten, T., Nielsen, L. B., Jorgensen, S., Kjaergaard, H. G., Canagaratna, M., Dal Maso, M., Berndt, T., Petaja, T., Wahner, A., Kerminen, V. M., Kulmala, M., Worsnop, D. R., Wildt, J., and Mentel, T. F.: A large source of low-volatility secondary organic aerosol, Nature, 506, 476–479, doi:10.1038/nature13032, 2014.

Elbert, W., Taylor, P. E., Andreae, M. O., and Pöschl, U.: Contribution of fungi to primary biogenic aerosols in the atmosphere: wet and dry discharged spores, carbohydrates, and inorganic ions, Atmos. Chem. Phys., 7, 4569–4588, doi:10.5194/acp-7-4569-2007, 2007.

Ervens, B., Turpin, B. J., and Weber, R. J.: Secondary organic aerosol formation in cloud droplets and aqueous particles (aqSOA): a review of laboratory, field and model studies, Atmos. Chem. Phys., 11, 11069–11102, doi:10.5194/acp-11-11069-2011, 2011.

Farmer, D. K., Matsunaga, A., Docherty, K. S., Surratt, J. D., Seinfeld, J. H., Ziemann, P. J., and Jimenez, J. L.: Response of an aerosol mass spectrometer to organonitrates and organosulfates and implications for atmospheric chemistry, P. Natl. Acad. Sci. USA, 107, 6670–6675, doi:10.1073/pnas.0912340107, 2010.

Fuzzi, S., Decesari, S., Facchini, M. C., Cavalli, F., Emblico, L., Mircea, M., Andreae, M. O., Trebs, I., Hoffer, A., Guyon, P., Artaxo, P., Rizzo, L. V., Lara, L. L., Pauliquevis, T., Maenhaut, W., Raes, N., Chi, X. G., Mayol-Bracero, O. L., Soto-Garcia, L. L., Claeys, M., Kourtchev, I., Rissler, J., Swietlicki, E., Tagliavini, E., Schkolnik, G., Falkovich, A. H., Rudich, Y., Fisch, G., and Gatti, L. V.: Overview of the inorganic and organic composition of size-segregated aerosol in Rondonia, Brazil, from the biomass-burning period to the onset of the wet season, J. Geophys. Res., 112, D01201, doi:10.1029/2005JD006741, 2007.

Gerab, F., Artaxo, P., Gillett, R., and Ayers, G.: PIXE, PIGE and ion chromatography of aerosol particles from northeast Amazon Basin, Nucl. Instrum. Meth. B, 136, 955–960, 1998.

Graham, B., Guyon, P., Maenhaut, W., Taylor, P. E., Ebert, M., Matthias-Maser, S., Mayol-Bracero, O. L., Godoi, R. H. M., Artaxo, P., Meixner, F. X., Moura, M. A. L., Rocha, C., Van Grieken, R., Glovsky, M. M., Flagan, R. C., and Andreae, M. O.: Composition

and diurnal variability of the natural Amazonian aerosol, J. Geophys. Res., 108, 4765, doi:10.1029/2003JD004049, 2003a.

Graham, B., Guyon, P., Taylor, P. E., Artaxo, P., Maenhaut, W., Glovsky, M. M., Flagan, R. C., and Andreae, M. O.: Organic compounds present in the natural Amazonian aerosol: characterization by gas chromatography-mass spectrometry, J. Geophys. Res., 108, 4766, doi:10.1029/2003jd003990, 2003b.

Gunthe, S. S., King, S. M., Rose, D., Chen, Q., Roldin, P., Farmer, D. K., Jimenez, J. L., Artaxo, P., Andreae, M. O., Martin, S. T., and Pöschl, U.: Cloud condensation nuclei in pristine tropical rainforest air of Amazonia: size-resolved measurements and modeling of atmospheric aerosol composition and CCN activity, Atmos. Chem. Phys., 9, 7551–7575, doi:10.5194/acp-9-7551-2009, 2009.

IPCC: Climate Change 2013: The Physical Science Basis. Contribution of Working Group I to the Fifth Assessment Report of the Intergovernmental Panel on Climate Change, edited by: Stocker, T. F., Qin, D., Plattner, G.-K., Tignor, M., Allen, S. K., Boschung, J., Nauels, A., Xia, Y., Bex, V., and Midgley, P. M., Cambridge University Press, Cambridge, United Kingdom and New York, NY, USA, 1535 pp., 2013.

Jimenez, J. L., Canagaratna, M. R., Donahue, N. M., Prevot, A. S. H., Zhang, Q., Kroll, J. H., DeCarlo, P. F., Allan, J. D., Coe, H., Ng, N. L., Aiken, A. C., Docherty, K. S., Ulbrich, I. M., Grieshop, A. P., Robinson, A. L., Duplissy, J., Smith, J. D., Wilson, K. R., Lanz, V. A., Hueglin, C., Sun, Y. L., Tian, J., Laaksonen, A., Raatikainen, T., Rautiainen, J., Vaattovaara, P., Ehn, M., Kulmala, M., Tomlinson, J. M., Collins, D. R., Cubison, M. J., Dunlea, E. J., Huffman, J. A., Onasch, T. B., Alfarra, M. R., Williams, P. I., Bower, K., Kondo, Y., Schneider, J., Drewnick, F., Borrmann, S., Weimer, S., Demerjian, K., Salcedo, D., Cottrell, L., Griffin, R., Takami, A., Miyoshi, T., Hatakeyama, S., Shimono, A., Sun, J. Y., Zhang, Y. M., Dzepina, K., Kimmel, J. R., Sueper, D., Jayne, J. T., Herndon, S. C., Trimborn, A. M., Williams, L. R., Wood, E. C., Middlebrook, A. M., Kolb, C. E., Baltensperger, U., and Worsnop, D. R.: Evolution of organic aerosols in the atmosphere, Science, 326, 1525–1529, doi:10.1126/science.1180353, 2009.

Karl, T., Guenther, A., Turnipseed, A., Tyndall, G., Artaxo, P., and Martin, S.: Rapid formation of isoprene photo-oxidation products observed in Amazonia, Atmos. Chem. Phys., 9, 7753–7767, doi:10.5194/acp-9-7753-2009, 2009.

Kiendler-Scharr, A., Zhang, Q., Hohaus, T., Kleist, E., Mensah, A., Mentel, T. F., Spindler, C., Uerlings, R., Tillmann, R., and Wildt, J.: Aerosol mass spectrometric features of biogenic

SOA: observations from a plant chamber and in rural atmospheric environments, Environ. Sci. Technol., 43, 8166–8172, doi:10.1021/es901420b, 2009.
Kostenidou, E., Lee, B. H., Engelhart, G. J., Pierce, J. R., and Pandis, S. N.: Mass spectra deconvolution of low, medium, and high volatility biogenic secondary organic aerosol, Environ. Sci. Technol., 43, 4884–4889, doi:10.1021/es803676g, 2009.
Kuhn, U., Ganzeveld, L., Thielmann, A., Dindorf, T., Schebeske, G., Welling, M., Sciare, J., Roberts, G., Meixner, F. X., Kesselmeier, J., Lelieveld, J., Kolle, O., Ciccioli, P., Lloyd, J., Trentmann, J., Artaxo, P., and Andreae, M. O.: Impact of Manaus City on the Amazon Green Ocean atmosphere: ozone production, precursor sensitivity and aerosol load, Atmos. Chem. Phys., 10, 9251–9282, doi:10.5194/acp-10-9251-2010, 2010.
Kuwata, M., Liu, Y., McKinney, K. A., and Martin, S. T.: Phase and acidity regulate the production of secondary organic material from isoprene photooxidation, in preparation, 2014.
Lim, Y. B., Tan, Y., Perri, M. J., Seitzinger, S. P., and Turpin, B. J.: Aqueous chemistry and its role in secondary organic aerosol (SOA) formation, Atmos. Chem. Phys., 10, 10521–10539, doi:10.5194/acp-10-10521-2010, 2010.
Lin, Y. H., Zhang, Z. F., Docherty, K. S., Zhang, H. F., Budisulistiorini, S. H., Rubitschun, C. L., Shaw, S. L., Knipping, E. M., Edgerton, E. S., Kleindienst, T. E., Gold, A., and Surratt, J. D.: Isoprene epoxydiols as precursors to secondary organic aerosol formation: acid-catalyzed reactive uptake studies with authentic compounds, Environ. Sci. Technol., 46, 250–258, doi:10.1021/es202554c, 2012.
Liu, S., Shilling, J. E., Song, C., Hiranuma, N., Zaveri, R. A., and Russell, L. M.: Hydrolysis of organonitrate functional groups in aerosol particles, Aerosol Sci. Technol., 46, 1359–1369, doi:10.1080/02786826.2012.716175, 2012.
Malm, W. C., Sisler, J. F., Huffman, D., Eldred, R. A., and Cahill, T. A.: Spatial and seasonal trends in particle concentration and optical extinction in the united states, J. Geophys. Res., 99, 1347–1370, 1994.
Martin, S. T., Andreae, M. O., Artaxo, P., Baumgardner, D., Chen, Q., Goldstein, A. H., Guenther, A., Heald, C. L., Mayol-Bracero, O. L., McMurry, P. H., Pauliquevis, T., Poschl, U., Prather, K. A., Roberts, G. C., Saleska, S. R., Dias, M. A. S., Spracklen, D. V., Swietlicki, E., and Trebs, I.: Sources and properties of amazonian aerosol particles, Rev. Geophys., 48, Rg2002, doi:10.1029/2008rg000280, 2010a.
Martin, S. T., Andreae, M. O., Althausen, D., Artaxo, P., Baars, H., Borrmann, S., Chen, Q., Farmer, D. K., Guenther, A., Gunthe, S. S., Jimenez, J. L., Karl, T., Longo, K., Manzi, A.,

Müller, T., Pauliquevis, T., Petters, M. D., Prenni, A. J., Pöschl, U., Rizzo, L. V., Schneider, J., Smith, J. N., Swietlicki, E., Tota, J., Wang, J., Wiedensohler, A., and Zorn, S. R.: An overview of the Amazonian Aerosol Characterization Experiment 2008 (AMAZE-08), Atmos. Chem. Phys., 10, 11415–11438, doi:10.5194/acp-10-11415-2010, 2010b.
Matthew, B. M., Middlebrook, A. M., and Onasch, T. B.: Collection efficiencies in an Aerodyne aerosol mass spectrometer as a function of particle phase for laboratory generated aerosols, Aerosol Sci. Technol., 42, 884–898, doi:10.1080/02786820802356797, 2008.
Middlebrook, A. M., Bahreini, R., Jimenez, J. L., and Canagaratna, M. R.: Evaluation of composition-dependent collection efficiencies for the Aerodyne aerosol mass spectrometer using field data, Aerosol Sci. Technol., 46, 258–271, doi:10.1080/02786826.2011.620041, 2012.
Ng, N. L., Canagaratna, M. R., Zhang, Q., Jimenez, J. L., Tian, J., Ulbrich, I. M., Kroll, J. H., Docherty, K. S., Chhabra, P. S., Bahreini, R., Murphy, S. M., Seinfeld, J. H., Hildebrandt, L., Donahue, N. M., DeCarlo, P. F., Lanz, V. A., Prévôt, A. S. H., Dinar, E., Rudich, Y., and Worsnop, D. R.: Organic aerosol components observed in Northern Hemispheric datasets from Aerosol Mass Spectrometry, Atmos. Chem. Phys., 10, 4625–4641, doi:10.5194/acp-10-4625-2010, 2010.
Ng, N. L., Canagaratna, M. R., Jimenez, J. L., Chhabra, P. S., Seinfeld, J. H., and Worsnop, D. R.: Changes in organic aerosol composition with aging inferred from aerosol mass spectra, Atmos. Chem. Phys., 11, 6465–6474, doi:10.5194/acp-11-6465-2011, 2011.
Nguyen, T. B., Coggon, M. M., Bates, K. H., Zhang, X., Schwantes, R. H., Schilling, K. A., Loza, C. L., Flagan, R. C., Wennberg, P. O., and Seinfeld, J. H.: Organic aerosol formation from the reactive uptake of isoprene epoxydiols (IEPOX) onto non-acidified inorganic seeds, Atmos. Chem. Phys., 14, 3497–3510, doi:10.5194/acp-14-3497-2014, 2014.
Paatero, P. and Tapper, U.: Positive matrix factorization – a nonnegative factor model with optimal utilization of error-estimates of data values, Environmetrics, 5, 111–126, doi:10.1002/env.3170050203, 1994.
Pankow, J. F.: An absorption-model of the gas aerosol partitioning involved in the formation of secondary organic aerosol, Atmos. Environ., 28, 189–193, 1994.
Petzold, A., Kramer, H., and Schonlinner, M.: Continuous measurement of atmospheric black carbon using a multi-angle absorption photometer, Environ. Sci. Pollut. R., 4, 78–82, 2002.
Pöhlker, C., Wiedemann, K. T., Sinha, B., Shiraiwa, M., Gunthe, S. S., Smith, M., Su, H., Artaxo, P., Chen, Q., Cheng, Y. F., Elbert, W., Gilles, M. K., Kilcoyne, A. L. D., Moffet, R. C.,

Weigand, M., Martin, S. T., Poeschl, U., and Andreae, M. O.: Biogenic potassium salt particles as seeds for secondary organic aerosol in the Amazon, Science, 337, 1075–1078, doi:10.1126/science.1223264, 2012.

Pöschl, U., Martin, S. T., Sinha, B., Chen, Q., Gunthe, S. S., Huffman, J. A., Borrmann, S., Farmer, D. K., Garland, R. M., Helas, G., Jimenez, J. L., King, S. M., Manzi, A., Mikhailov, E., Pauliquevis, T., Petters, M. D., Prenni, A. J., Roldin, P., Rose, D., Schneider, J., Su, H., Zorn, S. R., Artaxo, P., and Andreae, M. O.: Rainforest aerosols as biogenic nuclei of clouds and precipitation in the Amazon, Science, 329, 1513–1516, doi:10.1126/science.1191056, 2010.

Prenni, A. J., Petters, M. D., Kreidenweis, S. M., Heald, C. L., Martin, S. T., Artaxo, P., Garland, R. M., Wollny, A. G., and Poschl, U.: Relative roles of biogenic emissions and Saharan dust as ice nuclei in the Amazon Basin, Nat. Geosci., 2, 401–404, doi:10.1038/Ngeo517, 2009.

Rizzo, L. V., Artaxo, P., Müller, T., Wiedensohler, A., Paixão, M., Cirino, G. G., Arana, A., Swietlicki, E., Roldin, P., Fors, E. O., Wiedemann, K. T., Leal, L. S. M., and Kulmala, M.: Long term measurements of aerosol optical properties at a primary forest site in Amazonia, Atmos. Chem. Phys., 13, 2391–2413, doi:10.5194/acp-13-2391-2013, 2013.

Robinson, N. H., Hamilton, J. F., Allan, J. D., Langford, B., Oram, D. E., Chen, Q., Docherty, K., Farmer, D. K., Jimenez, J. L., Ward, M. W., Hewitt, C. N., Barley, M. H., Jenkin, M. E., Rickard, A. R., Martin, S. T., McFiggans, G., and Coe, H.: Evidence for a significant proportion of Secondary Organic Aerosol from isoprene above a maritime tropical forest, Atmos. Chem. Phys., 11, 1039–1050, doi:10.5194/acp-11-1039-2011, 2011.

Schneider, J., Freutel, F., Zorn, S. R., Chen, Q., Farmer, D. K., Jimenez, J. L., Martin, S. T., Artaxo, P., Wiedensohler, A., and Borrmann, S.: Mass-spectrometric identification of primary biological particle markers and application to pristine submicron aerosol measurements in Amazonia, Atmos. Chem. Phys., 11, 11415–11429, doi:10.5194/acp-11-11415-2011, 2011.

Shilling, J. E., Chen, Q., King, S. M., Rosenoern, T., Kroll, J. H., Worsnop, D. R., DeCarlo, P. F., Aiken, A. C., Sueper, D., Jimenez, J. L., and Martin, S. T.: Loading-dependent elemental composition of α-pinene SOA particles, Atmos. Chem. Phys., 9, 771–782, doi:10.5194/acp-9-771-2009, 2009.

Slowik, J. G., Brook, J., Chang, R. Y.-W., Evans, G. J., Hayden, K., Jeong, C.-H., Li, S.-M., Liggio, J., Liu, P. S. K., McGuire, M., Mihele, C., Sjostedt, S., Vlasenko, A., and Abbatt, J. P. D.: Photochemical processing of organic aerosol at nearby continental sites: contrast between

urban plumes and regional aerosol, Atmos. Chem. Phys., 11, 2991–3006, doi:10.5194/acp-11-2991-2011, 2011.

Surratt, J. D., Chan, A. W. H., Eddingsaas, N. C., Chan, M. N., Loza, C. L., Kwan, A. J., Hersey, S. P., Flagan, R. C., Wennberg, P. O., and Seinfeld, J. H.: Reactive intermediates revealed in secondary organic aerosol formation from isoprene, P. Natl. Acad. Sci. USA, 107, 6640–6645, doi:10.1073/pnas.0911114107, 2010.

Talbot, R. W., Andreae, M. O., Andreae, T. W., and Harriss, R. C.: Regional aerosol chemistry of the Amazon Basin during the dry season, J. Geophys. Res., 93, 1499–1508, 1988.

Talbot, R. W., Andreae, M. O., Berresheim, H., Artaxo, P., Garstang, M., Harriss, R. C., Beecher, K. M., and Li, S. M.: Aerosol chemistry during the wet season in central amazonia: the influence of long-range transport, J. Geophys. Res., 95, 16955–16969, 1990.

Trebs, I., Metzger, S., Meixner, F. X., Helas, G. N., Hoffer, A., Rudich, Y., Falkovich, A. H., Moura, M. A. L., da Silva, R. S., Artaxo, P., Slanina, J., and Andreae, M. O.: The NH_4^+-NO_3^--Cl^--SO_4^{2-}-H_2O aerosol system and its gas phase precursors at a pasture site in the Amazon Basin: how relevant are mineral cations and soluble organic acids?, J. Geophys. Res., 110, D07303, doi:10.1029/2004JD005478, 2005.

Ulbrich, I. M., Canagaratna, M. R., Zhang, Q., Worsnop, D. R., and Jimenez, J. L.: Interpretation of organic components from Positive Matrix Factorization of aerosol mass spectrometric data, Atmos. Chem. Phys., 9, 2891–2918, doi:10.5194/acp-9-2891-2009, 2009.

Vaden, T. D., Imre, D., Beranek, J., Shrivastava, M., and Zelenyuk, A.: Evaporation kinetics and phase of laboratory and ambient secondary organic aerosol, P. Natl. Acad. Sci. USA, 108, 2190–2195, doi:10.1073/pnas.1013391108, 2011.

Zhang, Q., Alfarra, M. R., Worsnop, D. R., Allan, J. D., Coe, H., Canagaratna, M. R., and Jimenez, J. L.: Deconvolution and quantification of hydrocarbon-like and oxygenated organic aerosols based on aerosol mass spectrometry, Environ. Sci. Technol., 39, 4938–4952, doi:10.1021/es048568l, 2005.

Zhang, Q., Jimenez, J. L., Canagaratna, M. R., Ulbrich, I. M., Ng, N. L., Worsnop, D. R., and Sun, Y. L.: Understanding atmospheric organic aerosols via factor analysis of aerosol mass spectrometry: a review, Anal. Bioanal. Chem., 401, 3045–3067, doi:10.1007/s00216-011-5355-y, 2011.

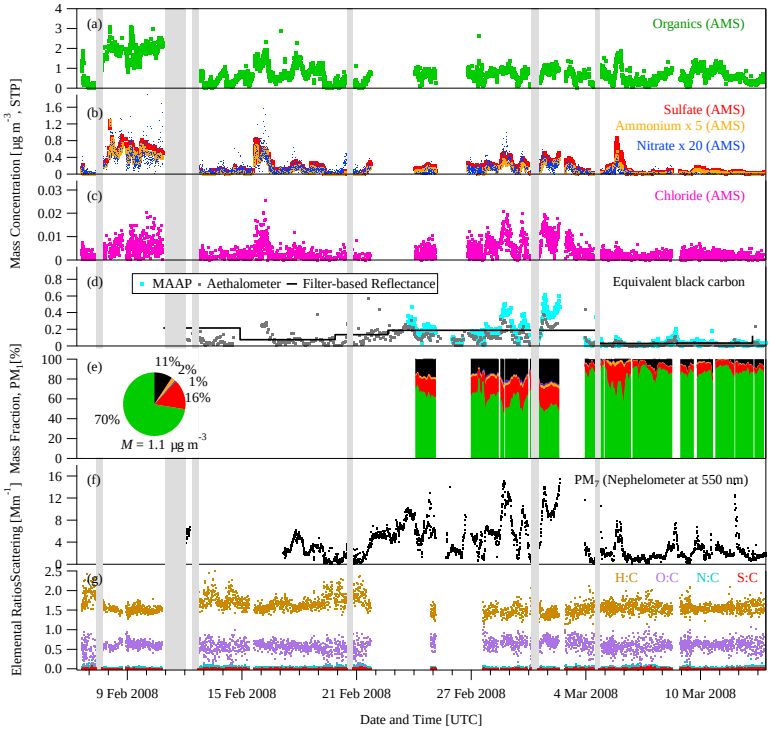

Discussion Paper | Discussion Paper | Discussion Paper | Discussion Paper |

Figure 1. Time series of observations during AMAZE-08. **(a–c)** Organic, sulfate, ammonium, nitrate, and chloride mass concentrations measured by AMS. **(d)** Black-carbon-equivalent mass concentrations measured by filter-based reflectance (fine-mode) analysis as well as optically derived by MAAP (637 nm) and aethalometer (660 nm) measurements. **(e)** Component mass fractions of **(a)** to **(d)**. For **(d)**, MAAP data were used. The inset pie chart represents the campaign average. **(f)** Scattering coefficient measured by nephelometry at 550 nm. Only particles of 7 µm and smaller passed through the sampling inlet. **(g)** Elemental ratios O : C, H : C, N : C, and S : C for the submicron organic particles, as determined by high-resolution AMS data. Except for **(f)**, the data represent the submicron or fine-mode fraction of the ambient particle population. Concentrations are normalized to STP conditions (see main text). Periods in gray were influenced by local generator exhaust plume during times of local wind reversal and were excluded from the shown data sets and analysis.

Discussion Paper | Discussion Paper | Discussion Paper | Discussion Paper |

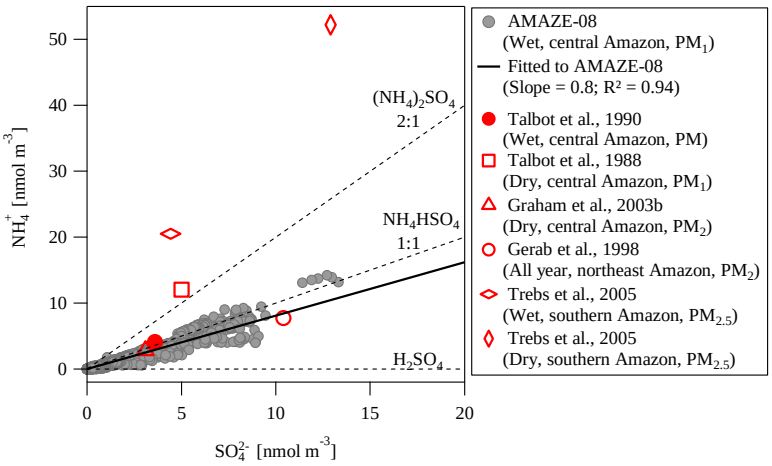

Figure 2. Scatter plot of ammonium and sulfate mass concentrations (gray circles). The red symbols show campaign-average values reported in the literature for other measurements in the Amazon Basin, both in the wet and dry seasons.

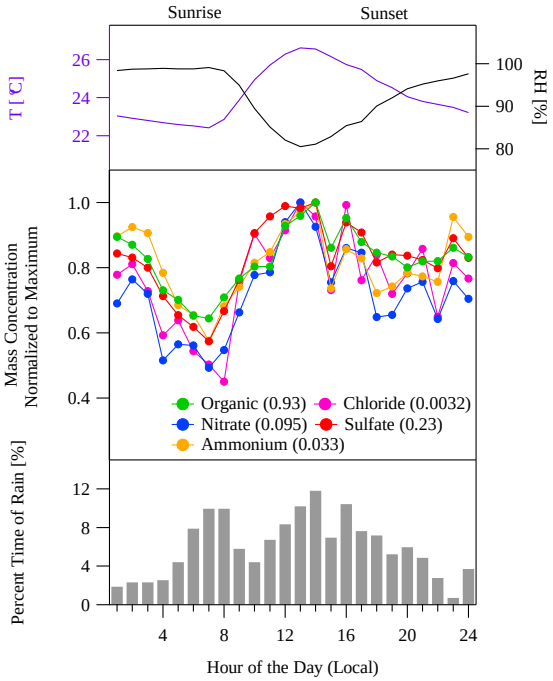

Figure 3. Diel profiles of (top) the temperature and relative humidity at the top of the measurement tower, (middle) normalized AMS-measured speciated mass concentrations (maximum concentrations in $\mu g\,m^{-3}$ (STP) are shown in parentheses), and (bottom) percent occurrence of rain. Data represent mean values.

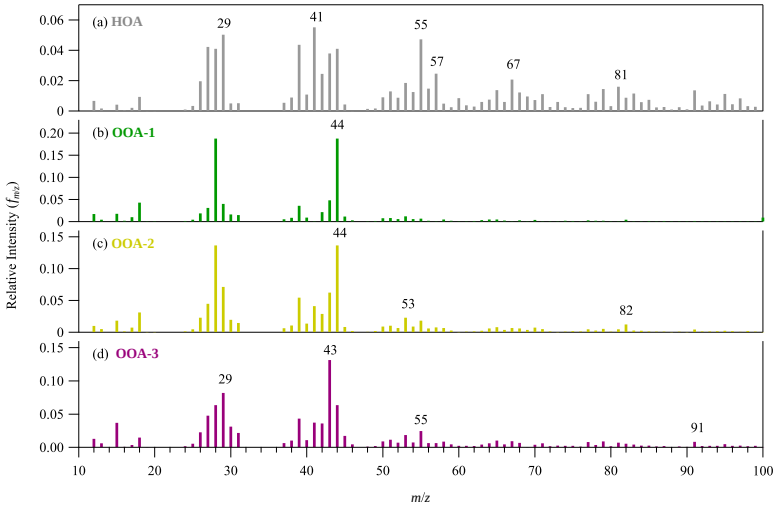

Figure 4. Statistical factors HOA, OOA-1, OOA-2, and OOA-3 identified by PMF analysis.

Discussion Paper | Discussion Paper | Discussion Paper | Discussion Paper |

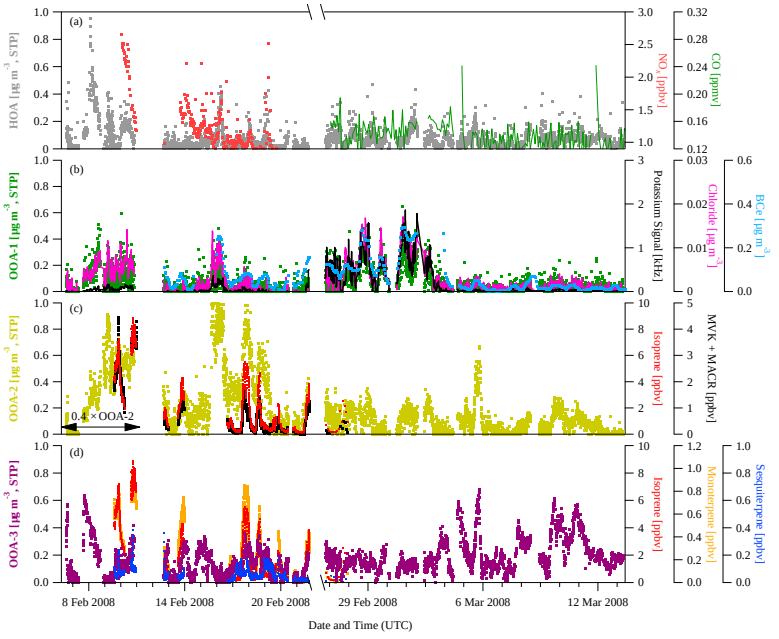

Figure 5. Time series of mass concentrations for the statistical factors HOA, OOA-1, OOA-2, and OOA-3 (left axes) and time series of the concentrations of tracer species, including NO_x, CO, AMS chloride, AMS potassium, aethalometer black-carbon, methyl vinyl ketone + methacrolein, isoprene, monoterpenes, and sesquiterpenes (right axes). The BVOCs were measured by PTR-MS (Karl et al., 2009).

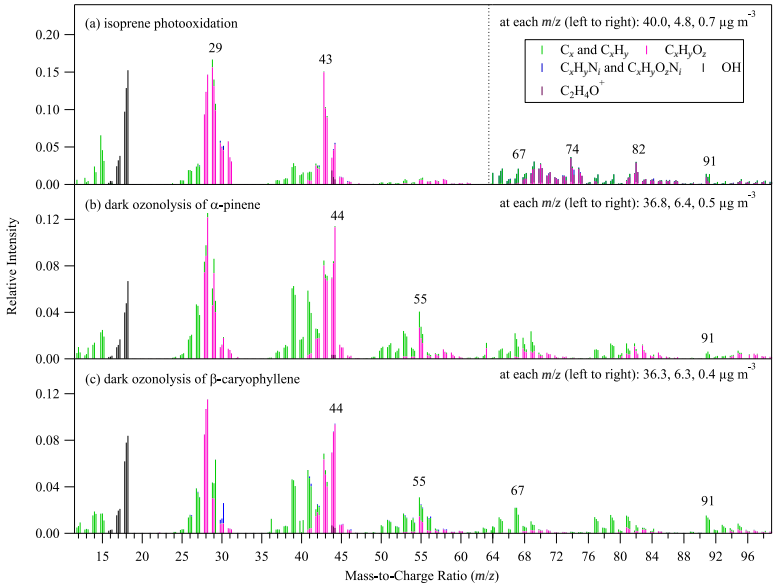

Figure 6. High-resolution mass spectra of secondary organic material produced in the Harvard Environmental Chamber by the oxidation of biogenic volatile organic compounds for < 1 ppbv NO_x. For isoprene photooxidation, the relative intensities of ions having $m/z > 63$ were multiplied by 10. The intensity at each unit-mass resolution is color-coded by the contribution of different ion families, as determined from analysis of the high-resolution spectra (Shilling et al., 2009). The relative intensities of the OH family were derived from the intensity of CO_2^+ based on calibrations described in Chen et al. (2011).

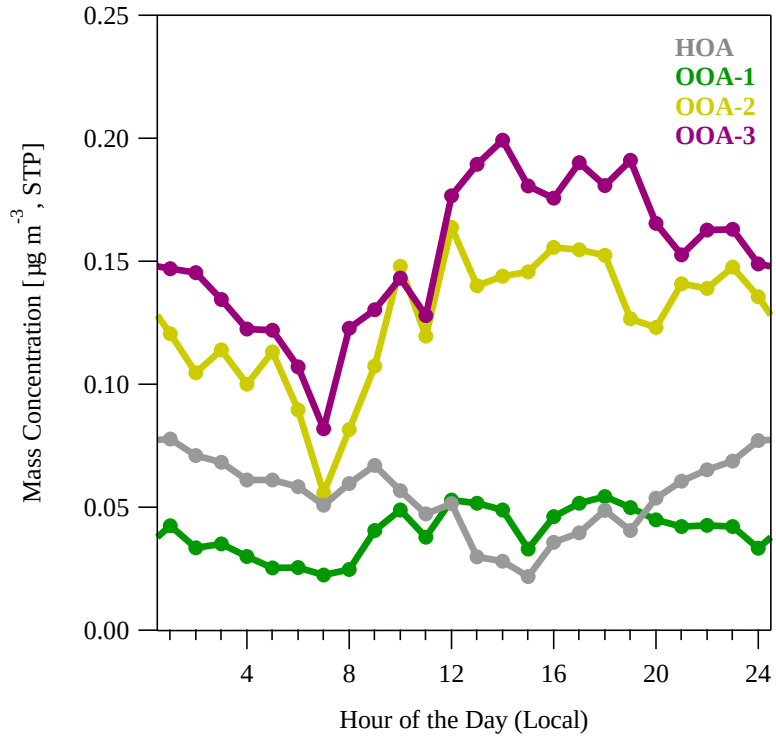

Figure 7. Diel profiles of the campaign-average mass concentrations of the statistical factors HOA, OOA-1, OOA-2, and OOA-3.

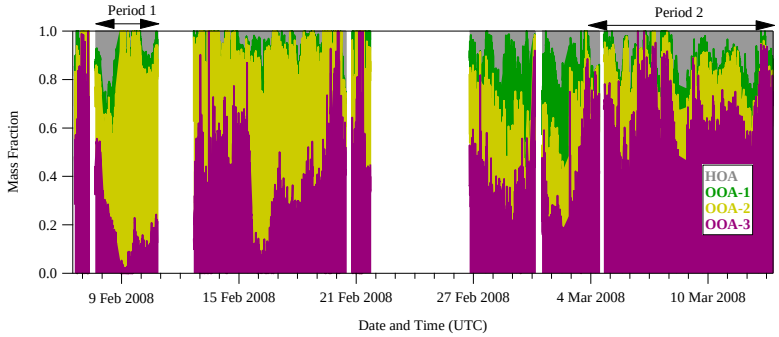

Figure 8. Time series of the fractional contribution by each of the four statistical factors identified by PMF analysis to the submicron organic particle mass concentrations.

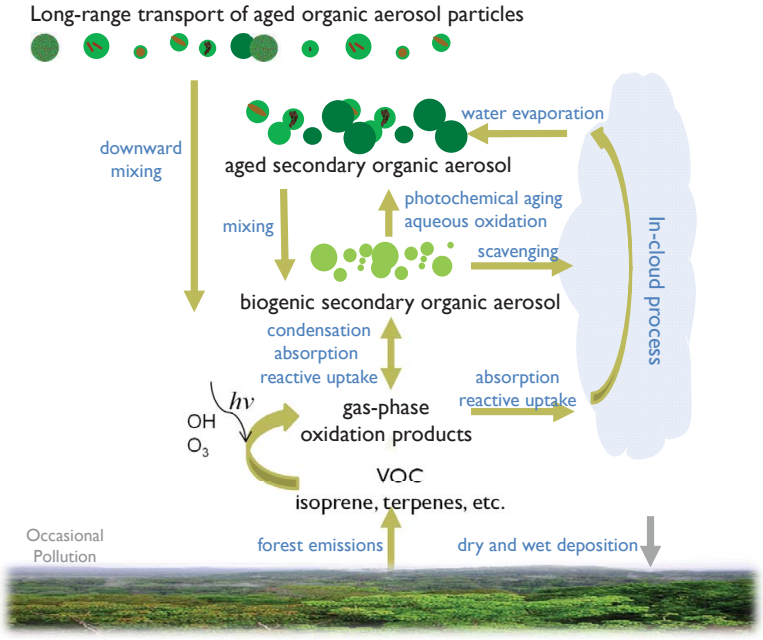

Figure 9. Processes depicted for the wet season concerning the production and further reactions of secondary organic material in the submicron size fraction of the Amazonian particle population.